Spirals in a reaction-diffusion system: Dependence of wave dynamics on excitability

Dhriti Mahanta, Nirmali Prabha Das, and Sumana Dutta*
Department of Chemistry, Indian Institute of Technology Guwahati, Guwahati 781039, India

(Received 26 July 2017; published 5 February 2018)

A detailed study of the effects of excitability of the Belousov-Zhabotinsky (BZ) reaction on spiral wave properties has been carried out. Using the Oregonator model, we explore the various regimes of wave activity, from sustained oscillations to wave damping, as the system undergoes a Hopf bifurcation, that is achieved by varying the excitability parameter, ϵ. We also discover a short range of parameter values where random oscillations are observed. With an increase in the value of ϵ, the frequency of the wave decreases exponentially, as the dimension of the spiral core expands. These numerical results are confirmed by carrying out experiments in thin layers of the BZ system, where the excitability is changed by varying the concentrations of the reactant species. Effect of reactant concentrations on wave properties like time period and wavelength are also explored in detail. Drifting and meandering spirals are found in the parameter space under investigation, with the excitability affecting the tip trajectory in a way predicted by the numerical studies. This study acts as a quantitative evidence of the relationship between the excitability parameter, ϵ, and the substrate concentrations.

DOI: 10.1103/PhysRevE.97.022206

I. INTRODUCTION

Rotating spiral waves have been observed ubiquitously in thin layers of excitable media like aggregating slime mold [1], cardiac tissue [2,3], frog oocyte [4], chemical reactions [5–7], etc. Spirals of electrical activity have been suggested to be responsible for cardiac arrhythmias, instabilities of which may further lead to ventricular fibrillation, the leading cause of heart failure in the modern world [2,8,9]. The first experimental evidence of spiral waves in a reaction diffusion system was found in the Belousov-Zhabotinsky (BZ) reaction [10]. Since then the BZ system has been a subject of particular interest due to its resemblance to other excitable systems in nature that sustain spiral waves.

A significant feature of spiral waves is the spiral center or core, the small area around which the wave rotates. Intensive investigation has shown that the dynamics of a spiral wave can be described by the motion of its tip. Initially it was believed that spiral tips follow circular paths until Winfree showed that under certain conditions, spirals can also be meandering (cycloidal curves) [11]. Since then, many results on meandering spiral waves have been published [12–15]. Experimental and theoretical analyses have shown that spiral tips can follow epicycloid orbits (flowerlike orbits with inward petals) or hypocycloid orbits (flowerlike orbits with outward petals) [5,16,17]. The dependence of the spiral tip on system parameters has been studied earlier in numerical simulations using reaction diffusion models, especially the Oregonator model [11,18]. Some other studies report the effects of the concentration of the inorganic acid on the geometry of the spiral [19,20]. It was found that in highly acidic conditions, spirals are Archimedean, whereas there occur deviations from the trend with decreasing acidity.

In this paper, we investigate the effects of excitability on the wave nature of the spirals. The Oregonator model of the BZ reaction system is chosen for our studies. By changing the value of the parameters, we are able to change the excitability of the system. We show that there is a strong dependence of the nature of the phase portrait, and hence the oscillatory character of the system, on ϵ, a parameter of the model. Also, the changes in spiral wave characteristics with ϵ are studied in detail.

To confirm our numerical results, we carry out experiments in thin layers of the Ferroin-catalyzed BZ system. We explore in detail the effect of substrate concentration on the dynamics of spiral waves. The concentrations of the reactants are varied in a controlled manner to monitor how the primary wave characteristics, like wavelengths and time periods, change. Also, we methodically study the tip trajectory of the spiral waves and are able to find a trend in the properties of the trajectory with the changing concentration of the reactants. Our experimental results are able to verify some earlier mathematical conclusions drawn about the Oregonator model that relates it to the actual concentration of the chemical species in the reaction. We show that such relationships are not restricted to the average wave properties alone, but also to the dynamics of the spiral tip.

II. MODEL

The Oregonator model, first proposed by Field and Noyes [21], is widely used to study spatiotemporal pattern formation in the BZ reaction. The model in the presence of diffusion can be described as below:

$$\frac{du}{dt} = \frac{1}{\epsilon}\left(u(1-u) - \frac{f v(u-q)}{(q+u)}\right) + D_u \nabla^2 u, \qquad (1)$$

$$\frac{dv}{dt} = u - v + D_v \nabla^2 v. \qquad (2)$$

Here, the time dependent variables u and v are dimensionless forms corresponding to the concentrations of bromous acid

*sumana@iitg.ernet.in

 ©2018 American Physical Society

and the oxidized form of the metal catalyst, respectively, q and f are kinetic parameters, and $D_u = 1.0$, $D_v = 0.6$ are the respective diffusion coefficients of u and v. ϵ represents the ratio of the time scales of the dynamics of the fast and slow variables.

Winfree in one of his papers [11] suggested a relationship between ϵ and the concentrations of the different chemical species in the BZ reaction, which is as given below:

$$\epsilon = \frac{k_5}{k_3}\frac{[\text{organics}]}{[H^+][BrO_3^-]}, \tag{3}$$

where [organics] = [BrMA] + [MA] (MA stands for malonic acid), $k_5 = 0.4\ M^{-1}s^{-1}$, and $k_3 = 40\ M^{-2}s^{-1}$.

The value of ϵ for any set of reactant concentrations can be calculated from the above equation. Since this parameter relates directly to the experimental conditions, we focused our attention to a methodical study of the system for varying values of ϵ.

For our simulations, Eqs. (1) and (2) were integrated using a standard fourth-order Runge-Kutta method for a two dimensional lattice of 300 × 300 grid points having zero flux boundaries along all the four walls. A time step of $dt = 0.001$ and a grid spacing of $dx = 0.1$ were employed. The above set of conditions can sustain spirals depending upon the values of ϵ, f, and q. Spirals were generated using the same initial conditions as in [11]. The tip of the spiral was identified as the isoconcentration points of u and v.

III. NUMERICAL RESULTS

Simulations were performed varying ϵ from 0.002 to 0.50. In Figs. 1(a)–1(c), snapshots of spiral waves for three different values of ϵ are depicted. The figures show that the frequency of the spiral wave decreases with an increase in ϵ. Figure 1(d) is a representative time-space plot which is created by stacking a cross section [yellow line in Fig. 1(b)] of the time-lapse snapshots of the system. The fish-bone shape of the time-space plot, with the phase difference between the lines going on either side from the center, confirms the presence of the spiral.

In order to study the detailed dynamics of the spiral waves we analyzed the tip trajectories for different values of ϵ. It was found that depending on the value of the kinetic terms and ϵ, the tip either follows a circular path or meanders, giving rise to a flowerlike pattern with petals of varying size. For parameter values $f = 2.0$ and $q = 0.002$ and ϵ varying in the range of 0.002 to 0.06, the spiral meanders with outward petals. The trajectories of the spiral tip for some of the ϵ values are shown in Fig. 2. There is a marked increase in the core size of the trajectories with increasing value of ϵ. For higher values of ϵ, the petals become very large and merge to give almost circular trajectories.

The time periods for different ϵ values are calculated from the corresponding time-space plots as depicted in Fig. 1(d). Figure 3 shows the plot of the inverse of the time period, which is closely related to the frequency, as a function of ϵ. It is observed that the frequency decays almost exponentially with the increase in ϵ values from 0.002 to 0.11. Above this value of ϵ, there is no formation of spirals, but only bulk oscillations and phase waves are obtained. In Fig. 3, the values of the time period beyond $\epsilon = 0.11$ are the periods of these phase

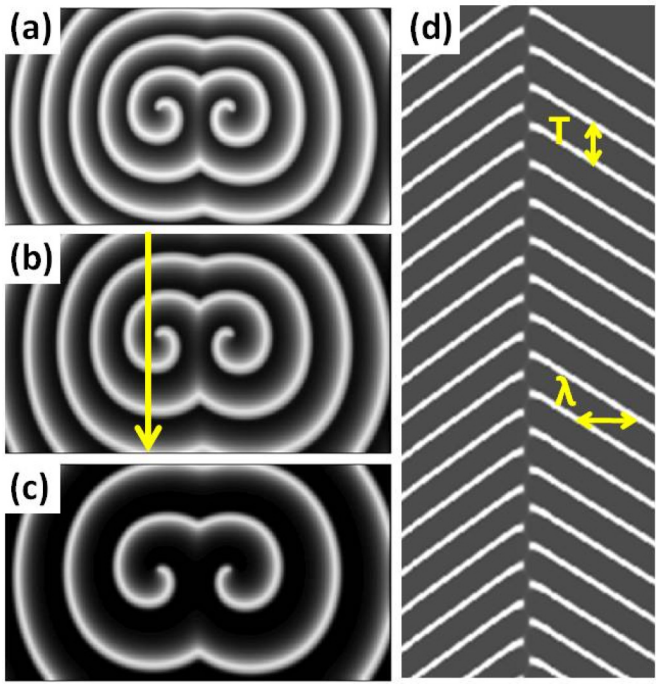

FIG. 1. Simulations of spiral waves generated using Oregonator model. (a)–(c) Snapshots of the stable spiral for three different values of ϵ: (a) 0.02, (b) 0.03, and (c) 0.04. $f = 2.0$ and $q = 0.002$ across all the simulations. (d) Time-space plot generated along the yellow arrow in (b), showing the time period T and the wavelength λ. Time increases from top to bottom.

waves. We have included them in this graph for a discussion of the oscillatory nature of the system with further increase of ϵ values. For ϵ just above 0.11 (∼0.12) we see the system undergoing random oscillations that finally reaches a stable nature after a long time. Similar nature is found for ϵ values around 0.15. In the intermediate range, however, only random oscillations are seen, and the system does not reach a state of regular oscillations even at $t = 5000$ time units. It is possible that they reach such a state after much longer times. The values

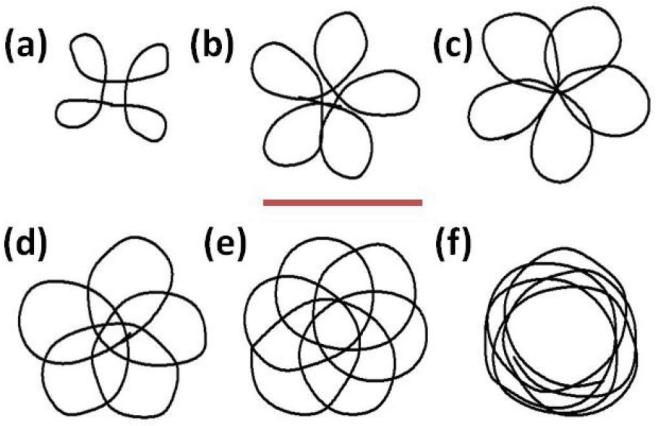

FIG. 2. Tip trajectories of spiral waves obtained from numerical simulation for ϵ values (a) 0.006, (b) 0.02, (c) 0.03, (d) 0.04, (e) 0.05, and (f) 0.06, respectively. Length of the bar shown below (b) is 3.6 space units.

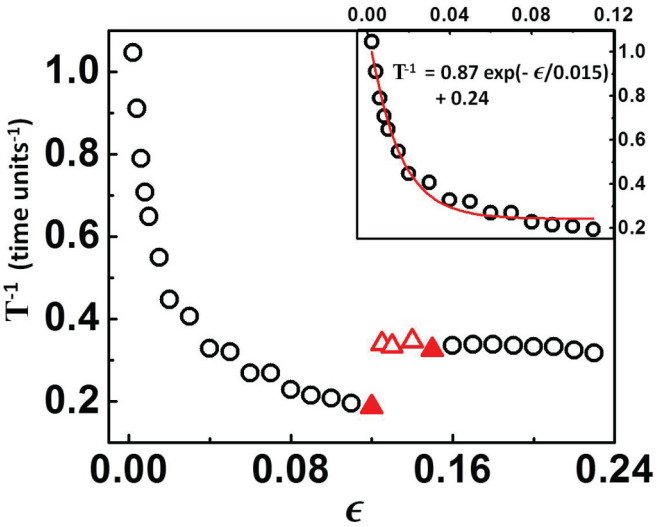

FIG. 3. Frequency of excitation waves in the Oregonator model as a function of ϵ. The black open circles are frequencies of stable oscillations, while the red triangles denote the average amplitude for a system displaying transience. In the beginning and end of this range, simulations for long times show that the system eventually reaches a state of stable oscillations. However, we have not been able to see any such phenomenon in the case of the data points given by open triangles. Here, the average value of its oscillating frequency has been reported. Inset shows the region for which spirals are obtained. The curve represents a fitting of the data as an exponential decay.

plotted in the figure for such states are averages over 30 oscillations. Just beyond $\epsilon = 0.12$, we observe a sudden jump in the frequency values. This jump marks the change in the spatial behavior of the system. For higher ϵ values, the frequency of the oscillations are almost constant, or vary very slightly.

We analyze the dynamics of the model on the phase plane for varying values of ϵ [Figs. 4(a)–4(e)]. Stable limit cycles are obtained for $\epsilon \leqslant 0.12$, followed by a regime of random oscillations, stable limit cycle, and finally fixed points. The frequency and amplitude of the oscillations also reflect the phase-space behavior. There are high amplitude, regular oscillations for $0.002 \leqslant \epsilon \leqslant 0.11$ [Fig. 4(f)]. This is the region where well-behaved spirals are formed. The corresponding limit cycles are shown in Fig. 4(a). In this parameter space, there is an exponential relationship between frequency and ϵ (Fig. 3). Beyond ϵ value 0.11, for a small parameter region, there is no existence of rotors, but the system initially oscillates with erratic amplitude as well as frequency [Figs. 4(b) and 4(g)] and stable oscillations are observed after a period of transience [Figs. 4(c) and 4(h)]. The phase space [Fig. 4(c)] shows that the system finally settles down to a limit cycle. As we further increase the value of the excitability parameter, through a short range of values ($0.12 < \epsilon < 0.15$), even though simulations were carried out for very long times ($t > 5000$ time units), we failed to observe any tendency of the system to reach stable oscillations. We carried out detailed analysis of the data to check for the existence of a limit cycle, but could not find any (see Supplemental Material [22]). The possibilities of a chaotic system in this parameter range cannot be ruled out but, since we are dealing with a two-dimensional system, no

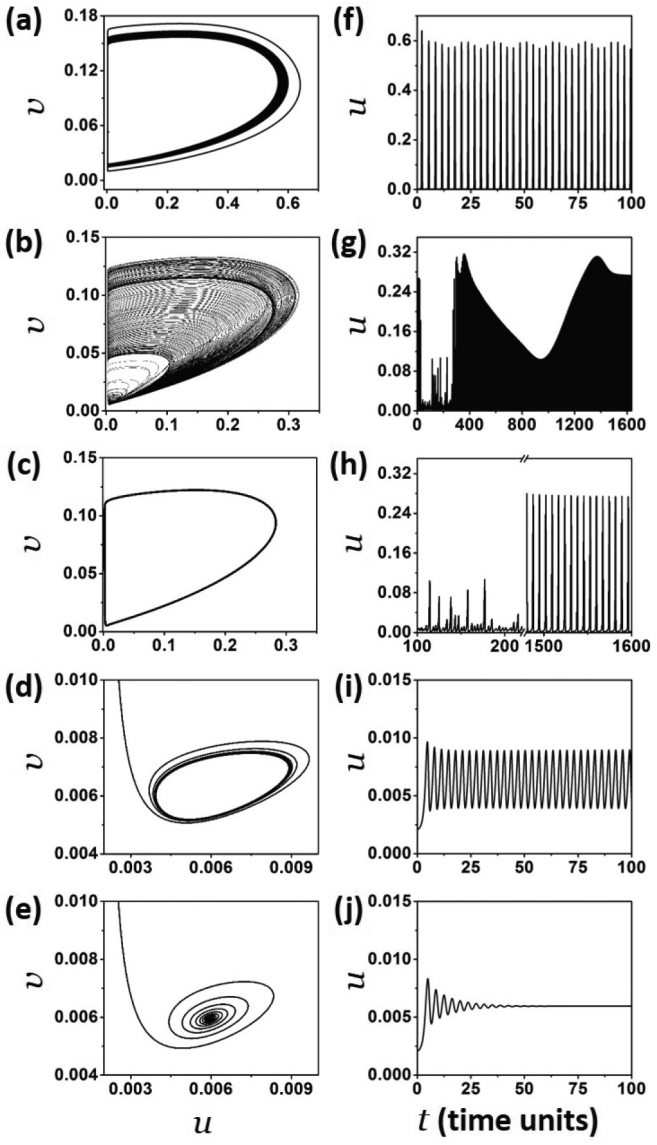

FIG. 4. Change in excitability with variation in epsilon values. (a)–(e) Dimensionless phase space diagrams and (f)–(j) oscillatory traces at different values of ϵ. In (a) and (f) $\epsilon = 0.04$, in (b), (c), (g), and (h) $\epsilon = 0.12$, in (d) and (i) $\epsilon = 0.20$, and in (e) and (j) $\epsilon = 0.28$. Panel (c) shows the limit cycle where the system finally settles down ($t = 1500$–1600 time units.)

such signatures could be detected. More detailed analysis of the three-dimensional Oregonator model will be required for this purpose.

At the end of this range, around $\epsilon \sim 0.15$, the transient system is again seen to reach a state of stable oscillations. After this, over a parameter range $0.16 \leqslant \epsilon < 0.24$, low-amplitude sustained oscillations are obtained [Fig. 4(i)]. This corresponds to the limit cycle behavior in Fig. 4(d). Finally, beyond $\epsilon = 0.23$, the system demonstrates damped oscillations. This can be seen in Figs. 4(e) and 4(j). The low amplitude oscillations quickly die down to reach a steady state [Fig. 4(j)]. This is reflected in the presence of a fixed point in the phase diagram [Fig. 4(e)]. The simulations were repeated for a single spiral and identical results were obtained. Since the excitability of the

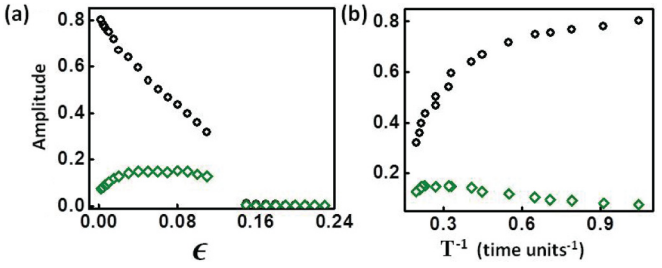

FIG. 5. Variation of amplitude of the oscillations with change in (a) ϵ value and (b) frequency. The values for the range ($0.11 < \epsilon < 0.15$), where random oscillations are observed, have been omitted. The black open circles denote values for u and olive diamonds are amplitudes in the variation of v.

medium depends so vividly on the parameter ϵ, we henceforth call it the excitability parameter.

It was observed that the amplitude of the oscillations in u reduce with the increase in the value of the excitability parameter, ϵ. We plot the variation of amplitude as a function of ϵ and the frequency of the waves (Fig. 5). A linear decrease in the amplitude of u is seen for those values of ϵ where spirals are formed ($\epsilon \leqslant 0.11$); however, beyond this range of values, there is a sudden drop in the amplitude. For higher values of epsilon ($\epsilon > 0.15$), the amplitude decreases very slowly, and eventually becomes zero for ($\epsilon > 0.23$). Beyond this parameter range, sustained oscillations are absent. With increase in the frequency, the amplitude in the oscillations of u show a logarithmic growth. Interestingly, amplitudes of variable v show a decreasing rate, after an initial increase, in both the cases (ϵ and T^{-1}). This change is however much less as compared to u. This may be due to the fact that v is the inhibitor, which is the slower variable, and, in the BZ, it denotes concentration of the metal catalyst, ferroin.

We summarize our numerical results in the form of a bifurcation diagram, generated as a function of the excitability parameter (Fig. 6). A system without diffusion shows two

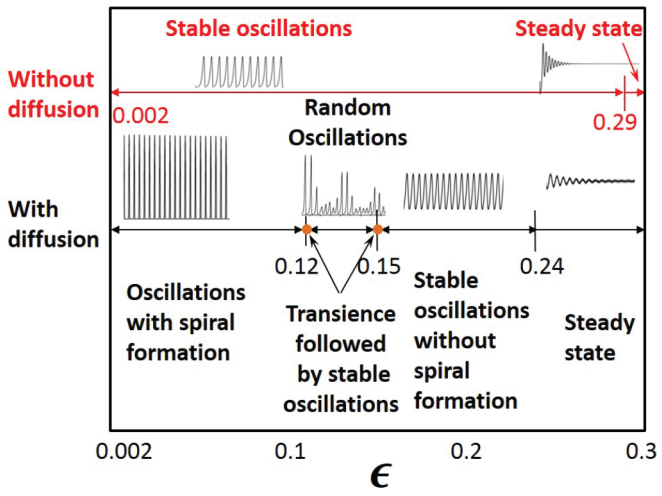

FIG. 6. Bifurcation diagram with (bottom, black) and without (top, red) diffusion. The change in the oscillatory nature of the system and corresponding wave nature with the variation in ϵ value has been depicted here.

regions: one region ($0.002 \leqslant \epsilon \leqslant 0.29$) demonstrates stable oscillations. In this region, there is an unstable fixed point surrounded by a stable limit cycle (see Supplemental Material [22]). The size of the limit cycle keeps on decreasing with the increase in ϵ value, till it engulfs the fixed point at around $\epsilon \sim 0.29$ and a stable fixed point is created. Beyond this value of the excitability parameter, there are no limit cycles and all oscillations damp down to a final steady state. This is a case of supercritical Hopf bifurcation. In the presence of diffusion, the system displays similar dynamics, but the Hopf bifurcation now sets in around $\epsilon \sim 0.24$. Also, there are some interesting variations in the nature of the excitation waves in the region where limit cycles are found. Spiral waves are obtained for low values of ϵ. They are followed by a short range of random oscillations, beyond which low-amplitude stable oscillations are observed. The limit cycle shrinks with the increase in the value of the excitability parameter, until a stable fixed point is created at the bifurcation point.

IV. EXPERIMENTAL SECTION

In this and later sections of our paper, we show that the influence of the excitability parameter on the dynamics of excitation waves can also be observed in real experimental systems. Our experiments were performed using thin layers of ferroin-catalyzed BZ reaction with malonic acid as the organic substrate. A series of experiments were carried out with concentrations of different reactants in the following range: $[H_2SO_4] = 0.16$–0.32 M, $[NaBrO_3] = 0.04$–0.12 M, and $[MA] = 0.04$–0.12 M. [Ferroin] $= 0.001$ M was kept constant for each reaction. Across these ranges of substrate concentrations spiral waves can be successfully initiated. Reaction mixtures outside the above range are either of high or low excitability. Therefore, only traveling waves or turbulent waves can be observed in the latter. The prepared BZ solution was transferred to a petri dish of 8 cm diameter. The thickness of the solution layer was about 2 mm. The mixture was swirled as the first oscillation completes and then kept undisturbed to attain a homogeneous state. A circular wave was generated by dipping, for a few seconds, the tip of a silver wire in the middle of the petri dish to prevent boundary effects. The main reason behind using the silver wire is the removal of the inhibitor Br^- from the vicinity as AgBr. The expanding circular wave front when cleaved results in the formation of a pair of spiral waves with two tips of opposite chirality. We then place a flat glass plate over the reaction mixture to eliminate the chances of aerial oxidation. The petri dish was covered to prevent any undesired hydrodynamics. In the above solution, oscillations continue for four hours or more. To capture images of our experiment, a charge coupled device (CCD) camera (mvBlueFOX 22a) was mounted above the system which was illuminated from below by a cold white light source. Snapshots were recorded onto a computer every two seconds and the data analyzed using in-house MATLAB codes.

V. RESULTS AND DISCUSSION

Figure 7 shows snapshots of spirals for six different sets of reaction mixtures. Each column corresponds to a particular concentration of H_2SO_4, while the concentrations of $NaBrO_3$

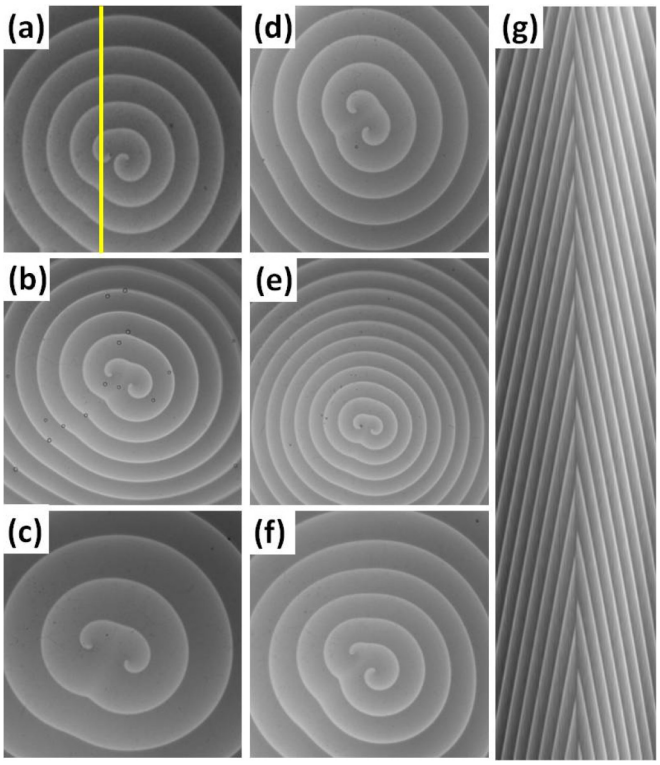

FIG. 7. Spirals in the BZ reaction. (a)–(f) Snapshots corresponding to different experiments with varying concentrations of the active chemical species. H_2SO_4 concentration across (a)–(c) is 0.2 M and across (d)–(f) is 0.28 M, respectively. $NaBrO_3$ concentration is 0.04 M in (a), (c), (d), (f) and 0.1 M in (b), (e). The concentration of malonic acid is 0.1 M in (c) and (f) and 0.04 M in all other experiments. Ferroin concentration is kept at 1 mM for each experiment. Each snapshot has an area of $4.8 \times 4.8\ cm^2$. (g) Time space plot generated from the cross section of the two dimensional images of the experiment depicted in (a), along the yellow line. It spans a time interval of 60 min. The ϵ values when calculated by Eq. (3) are found to be (a) 0.050, (b) 0.020, (c) 0.125, (d) 0.035, (e) 0.014, and (f) 0.089.

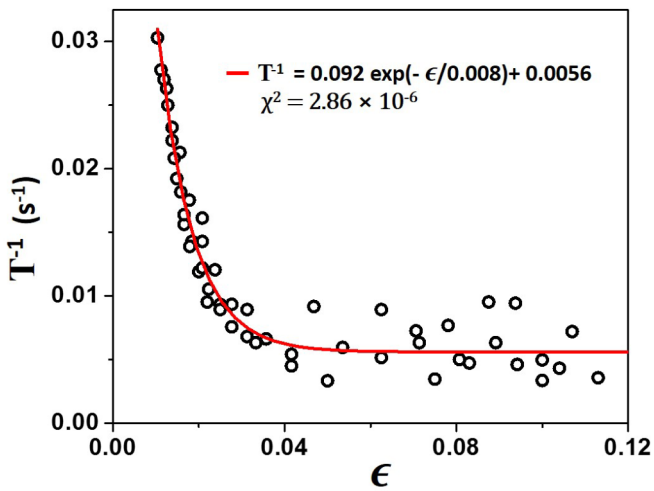

FIG. 8. Frequency of spirals in the BZ reaction as a function of the excitability parameter ϵ.

and MA are varied across the column. An observation of the spirals in Fig. 7 reveals that the dynamic behavior of the spiral waves depend on the initial concentrations of H_2SO_4, $NaBrO_3$, and MA. The frequency increases with increase in the concentration of H_2SO_4 and $NaBrO_3$, while the wavelength decreases. The changes due to MA seem to follow an opposite trend; however, the same is not so clear from these snapshots and further analysis is required.

In order to have a close comparison of our experiments with the numerical results, ϵ value for each experiment was calculated from Eq. (3) and plotted against frequency. Figure 8 shows that frequency decays exponentially with increasing value of ϵ. Thus it follows the same trend as shown in our simulations (Fig. 3).

The time period and wavelength of every experiment was measured from its corresponding time-space plot. The other important parameters of wave dynamics, viz. frequency and

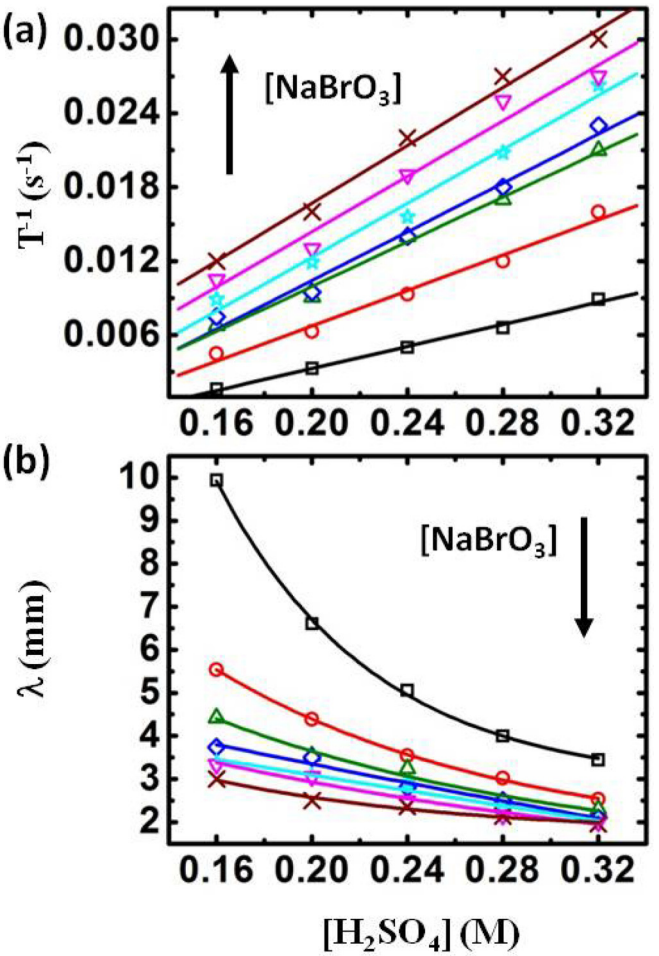

FIG. 9. Variation of wave properties with the concentrations of sulphuric acid and sodium bromate. (a) Frequency and (b) wavelength of the spiral wave as a function of H_2SO_4 concentration. Each curve corresponds to different concentrations of $NaBrO_3$: square (black) 0.04 M, circle (red) 0.06 M, upper triangle (olive) 0.08 M, diamond (blue) 0.09 M, star (cyan) 0.1 M, lower triangle (pink) 0.11 M, and cross (wine red) 0.12 M, respectively. Concentration of MA is kept constant at 0.04 M throughout these experiments and that of ferroin is maintained at 1 mM.

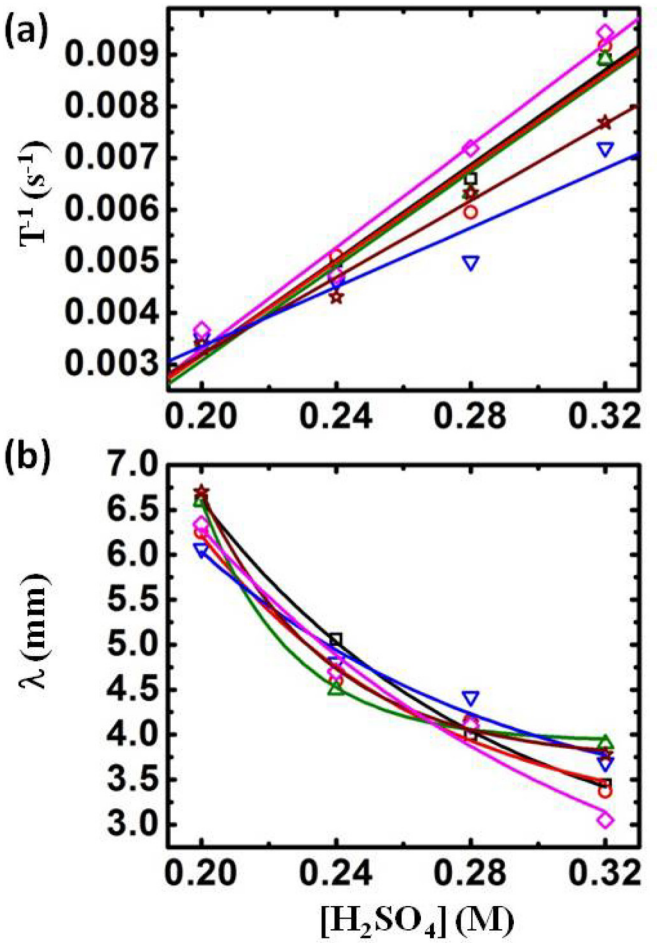

FIG. 10. Effect of malonic acid concentration on the properties of the spiral waves. (a) Frequency and (b) wavelength of the spiral wave as a function of H_2SO_4 concentration. Each curve corresponds to different [MA]: square (black) 0.06 M, circle (red) 0.08 M, upper triangle (olive) 0.09 M, lower triangle (blue) 0.1 M, star (wine red) 0.11 M, and diamond (pink) 0.12 M, respectively. [$NaBrO_3$] is kept constant at 0.04 M throughout these experiments and [ferroin] = 1 mM.

velocity, were also calculated from these values. The trends for the frequency and wavelength are summarized in Figs. 9 and 10. For an increase in the concentration of sulphuric acid, the frequency increases almost linearly, while the wavelength seems to decay exponentially (Fig. 9). With the increase in the concentrations of $NaBrO_3$, time period increases with a linear trend and the wavelengths of the spirals decrease (see Supplemental Material [22]). The velocities of the waves increase with the increase in the concentrations of the inorganic acid and the bromate. However, there is no such appreciable change in any of the parameters with change in the malonic acid concentration. This is evident from Fig. 10. At low concentrations of sulphuric acid, there is almost no difference in the frequency profile with the change in [MA]. Only at high [H_2SO_4], changes in the concentrations of MA result in a variation of the frequency of the waves, albeit with no such clear trend as in the case of $NaBrO_3$. Thus it can be said that the dynamical properties mostly depend on the concentrations of H_2SO_4 and $NaBrO_3$.

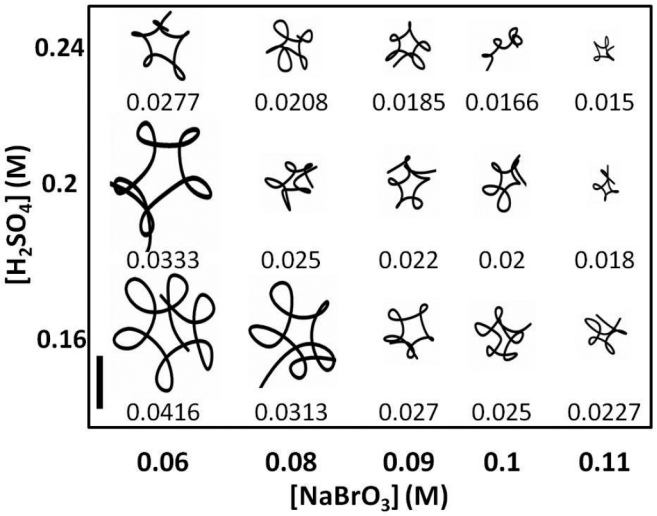

FIG. 11. Tip trajectories of spiral waves for different values of sulphuric acid and sodium bromate concentrations. Malonic acid concentration is kept fixed at 0.04 M and ferroin concentration at 1 mM. The number below each trajectory is the calculated value of ϵ. Length of the bar shown at the bottom left corner is 1 mm.

From simulations with the Oregonator model, it is seen that the spiral core can trace different types of floral trajectories whose nature and size depend on the kinetic parameters (Fig. 2). For our experiments with the BZ, we analyze the time-lapse snapshots of each experiment with some in-house MATLAB scripts to trace the trajectories of the spiral tips.

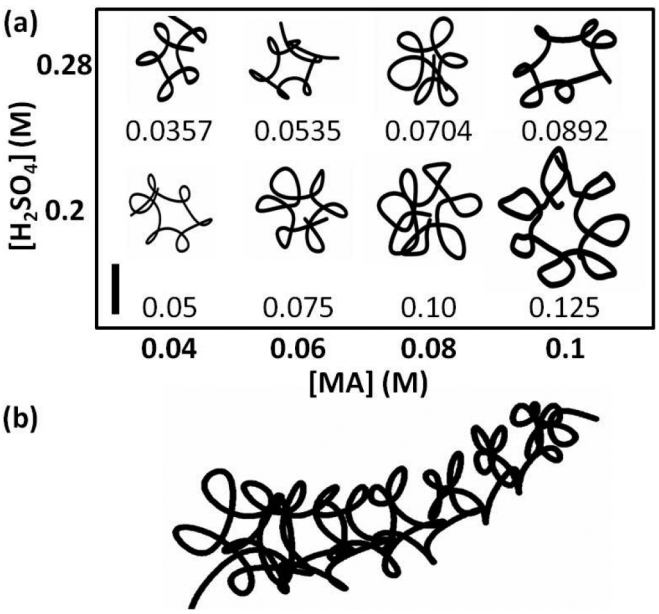

FIG. 12. Nature of trajectories of the spiral tip as a function of malonic acid concentration. (a) Trajectories with varying [H_2SO_4] and [MA]. In all the experiments, [$NaBrO_3$] = 0.04 M and [ferroin] = 1 mM. The calculated value of ϵ is noted below each trajectory. Black bar at the left bottom corner is of 1 mm length. (b) Trajectory of a meandering spiral wave for [$NaBrO_3$] = 0.08 M, [H_2SO_4] = 0.16 M, [MA] = 0.04 M, and [ferroin] = 1 mM.

Figures 11 and 12 show some examples of the spiral tip trajectories with increasing initial concentrations of the substrates. In all our experiments, we get hypocycloid curves, i.e., floral patterns with the petals facing outward. It is also observed that, for a particular concentration of H_2SO_4, and keeping [MA] constant, the number of petals decreases for increased concentrations of $NaBrO_3$ (Fig. 11). Simultaneously, the core size and the outer diameter of the trajectories also decrease. On the other hand, if we increase the concentrations of MA while keeping [H_2SO_4] and [$NaBrO_3$] constant, it is seen that the number of petals as well as the trajectory size increase [Fig. 12(a)]. Furthermore, for increasing concentrations of H_2SO_4, the size of the core as well as the outer diameter of the trajectory are seen to get smaller. For some specific concentrations of the reactants, it was found that the tip drifts from its original position with time, as can be seen in Fig. 12(b).

From Figs. 11 and 12 it is seen that the core size decreases with decrease in the value of ϵ. A similar trend was found in the results of our numerical simulations (Fig. 2). Thus changing the excitability can induce changes in the dynamics of a spiral wave that also leaves its mark on the nature of the tip trajectories.

VI. CONCLUSIONS

In this study of spiral waves in the two dimensional BZ system, we have shown that the initial concentrations of the substrates have a marked effect on the wave nature of the medium. Through experiments with thin layers of BZ solution as well as numerical simulations involving the Oregonator model, we have made a detailed quantitative analysis of the wave properties of the spirals from their time space plots. From the experiments, it was found that the period and wavelength decreased with increased concentrations of sulphuric acid and sodium bromate. The velocity and frequency of the waves had an exact opposite trend. In contrast, changes in the concentration of MA depicted no such significant changes of the wave properties. A detailed observation of the spiral tip trajectories also gave us newer insights into the spiral wave dynamics. The core of the spiral became smaller with increase in [H_2SO_4] and [$NaBrO_3$]. The trends are, however, opposite for the changes in [MA]. Hence we can surmise that the excitability increases with increasing H_2SO_4 and $NaBrO_3$ concentration, as is evident from higher frequency values, and the excitability is negatively affected by MA. Again, the wave characteristics are not so sensitive to the changes in MA concentration as they are to the changes in the concentrations of H_2SO_4 and $NaBrO_3$ as is evident from Figs. 9 and 10.

An important aspect of this study revolves around the Oregonator model parameter, ϵ, and the influence it has on the excitation dynamics of the BZ system. Our experiments and corresponding numerical simulations are a simple demonstration that the suggested relationship of ϵ with the concentrations of the reactants in the BZ system, as reported by earlier researchers, is valid not only in a "loose" qualitative sense, but in a very quantitative way. In our present study we show how the increase in this parameter brings about Hopf bifurcation in the system, as it passes from a regime of spiral waves, to a short phase of erratic oscillations, followed by phase waves, and finally collapses to a steady state. A range of parameter values where the system undergoes random oscillations has been discovered during this study. Further investigation of the three-variable Oregonator model may shed more light on the dynamics of the system in this regime. From our numerical simulations and experiments we have shown that there is an exponential decay in the frequency of the waves with increase in ϵ value, in the region where spirals are formed. The effect it has on the excitability of the medium and also in the spiral tip dynamics inspires us to call ϵ the excitability parameter.

The changes in the dynamics of the three dimensional scroll waves as functions of substrate concentrations will also be of much interest. Scroll wave turbulence and chaos in the BZ reaction are still elusive phenomena. Further studies with the 3D BZ system may enable us to achieve these by tweaking the excitability of the medium with a wise choice of reactant concentrations.

ACKNOWLEDGMENTS

This work was financially supported by the Science and Engineering Research Board, Government of India (Grant No. SB/S1/PC-19/2012).

[1] F. Siegert and C. J. Weijer, Physica D (Amsterdam) **49**, 224 (1991).
[2] R. A. Gray, A. M. Pertsov, and J. Jalife, Nature (London) **392**, 75 (1998).
[3] G. Bub, A. Shrier, and L. Glass, Phys. Rev. Lett. **88**, 058101 (2002).
[4] J. Lechleiter, S. Girard, E. Peralta, and D. Clapham, Science **252**, 123 (1991).
[5] A. T. Winfree, Science **175**, 634 (1972).
[6] S. Nettesheim, A. von Oertzen, H. H. Rotermund, and G. Ertl, J. Chem. Phys. **98**, 9977 (1993).
[7] F. Haudin, J. H. E. Cartwright, F. Brau, and A. De Wit, Proc. Natl. Acad. Sci. USA **111**, 17363 (2014).
[8] J. Jalife, R. A. Gray, G. E. Morley, and J. M. Davidenko, Chaos **8**, 79 (1998).
[9] L. Gaztañaga, F. E. Marchlinski, and B. P. Betenskya, Rev. Esp. Cardiol. **65**, 174 (2012).
[10] A. N. Zaikin and A. M. Zhabotinsky, Nature (London) **225**, 535 (1970).
[11] W. Jahnke, W. E. Skaggs, and A. T. Winfree, J. Phys. Chem. **93**, 740 (1989).
[12] G. Li, Q. Ouyang, V. Petrov, and H. L. Swinney, Phys. Rev. Lett. **77**, 2105 (1996).
[13] G. S. Skinner and H. L. Swinney, Physica D (Amsterdam) **48**, 1 (1991).
[14] M. Braune and H. Engel, Chem. Phys. Lett. **211**, 534 (1993).
[15] C. K. Tung and C. K. Chan, Phys. Rev. Lett. **89**, 248302 (2002).
[16] D. Barkley, Phys. Rev. Lett. **72**, 164 (1994).

[17] D. Barkley and I. G. Kevrekidis, Chaos **4**, 453 (1994).
[18] W. Jahnke and A. T. Winfree, Int. J. Bifurcat. Chaos **01**, 445 (1991).
[19] T. Plesser, S. C. Müller, and B. Hess, J. Phys. Chem. **94**, 7501 (1990).
[20] A. L. Belmonte, Q. Ouyang, and J. M. Flesselles, J. Phys. II (France) **7**, 1425 (1997).
[21] R. J. Field and R. M. Noyes, J. Chem. Phys. **60**, 1877 (1974).
[22] See Supplemental Material at http://link.aps.org/supplemental/10.1103/PhysRevE.97.022206 for additional analyses of numerical and experimental data.